Non-Thermal Activation of Reactions of Organic Molecules on Si(001)- Molecular Beam and Scanning Tunneling Microscopy Experiments

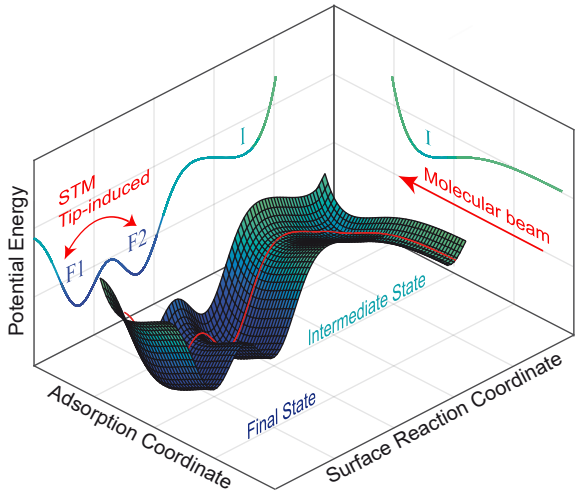

Dissertation zur Erlangung des Doktorgrades der Naturwissenschaften (Dr. rer. nat.)

dem

Fachbereich Physik

der Philipps-Universität Marburg
vorgelegt von

M.Sc.

Tamam Bo hamud

aus Safita, Syrien

Universitätsstadt Marburg, 2020

Eingereicht am:	15.02.2020
Als Dissertation angenommen am:	23.04.2020
Tag der mündliche Prüfung:	19.05.2020
Erstgutachter:	Prof. Dr. rer. nat. Ulrich Höfer
Zweitgutachter:	Prof. Dr. rer. nat. Michael Dürr
Hochschulkennziffer:	1180

Bo hamud, Tamam:
Non-Thermal Activation of Reactions of Organic Molecules on Si(001)- Molecular Beam and Scanning Tunneling Microscopy Experiments,
Philipps-Universität Marburg, Dissertation, 2020

Abstract

In the presented cumulative thesis, the reaction of different organic molecules on Si(001) surface are studied by using molecular beam techniques and scanning tunneling microscopy. The obtained results are discussed with a special focus on the dynamics of the reactions, the underlying potential energy curve, and the resulting possibility to control these reactions.

In the first part, we used molecular beam experiments to investigate the adsorption pathway of methanol, water, and acetylene on Si(001). We found that the adsorption of these three molecules proceeds via an intermediate state. The binding energy of the intermediate state ϵ_{d} depends on the configuration of the molecule and the resulting type of the intermediate. The difference between ϵ_{d} and the conversion barrier from the intermediate into the final state ϵ_{a}, is found to be $\epsilon_{\mathrm{d}} - \epsilon_{\mathrm{a}} = 0.37$, 0.36, 0.16 eV for methanol, water, and acetylene respectively. By comparing our results to well-established systems such as diethyl ether and ethylene on Si(001), we conclude on a low activated and fast conversion process from the intermediate into the final state for the three molecules. The conversion in the case of methanol and water proceeds via a proton-transfer reaction, which is known to be more facile than the O-C cleavage in the case of ether adsorption. The fast conversion for acetylene is attributed to the weak binding energy of the molecule in the intermediate, which involves the weaker three center bond between the π electrons of the molecule and the positively charged $\mathrm{D}_{\mathrm{down}}$ state of the silicon dimer in combination with a generally high reactivity of the triple bond. Based on these results on the energetics with substantial differences for these systems, a comprehensive study of the adsorption dynamics of these molecules was carried out by determining the dependence of the initial sticking coefficient s_0 on the kinetic energy of the adsorbing molecules, E_{kin}. We found that the main factor governing the adsorption dynamics is the type of the intermediate state, regardless the details of the adsorbed molecules or their possible further reaction, i.e., the conversion to the final state. The different dependence of the s_0 on the E_{kin} allows to control the reaction with respect to adsorption into the intermediate state.

In the second part of the thesis, a further manipulation of the adsorbates after the conversion from the intermediate into the final state is discussed. The system of diethyl ether on Si(001) is taken as an example as it shows two different configurations in the final state. Mutual conversions between the two configurations is observed by using scanning tunneling microscopy. This conversion between the two sub-states is

attributed to a field-assisted thermally activated hopping of the alkyl fragment of the cleaved diethyl ether on top of one Si dimer. The relative hopping rate shows clear dependence on the bias voltage, but remains constant when varying the tunneling current. This observation is attributed to a reduction of the energy barrier by depolarizing the C-Si bond by the electric field of the negative STM tip. The energetic contribution of the field was found to be at least 0.3 eV, which correlates well with the value of the electric field at the respective distance between tip and sample.

Zusammenfassung

In der vorliegenden kumulativen Dissertation wird die Reaktion verschiedener organischer Moleküle auf Si(001) untersucht. Zu diesem Zweck wurden Messungen an einer Molekularstrahlapparatur und einem temperaturvariablen Rastertunnelmikroskop durchgeführt. Im Fokus stand dabei die untersuchung der Kinetik und der Dynamik der jeweiligen Adsorptionsprozesse, um diese zu verstehen und zu kontrollieren, sowie gezielt auf andere Systeme übertragen zu können.

Im ersten Teil der Arbeit wurden anhand von Molekularstrahlexperimenten die Adsorptionsprozesse von Methanol sowie Wasser und Acetylen auf Si(001) untersucht. Alle drei Systeme weisen einen Adsorptionsweg auf, der über einen Zwischenzustand verläuft. Die Bindungsenergie dieses Zwischenzustands ϵ_d hängt von der jeweiligen Konfiguration des Moleküls, sowie von der an der Adsorption beteiligten funktionellen Gruppe ab. Die Differenz zwischen ϵ_d und der Konversionsbarriere vom Zwischen- in den Endzustand ϵ_a wurde zu $\epsilon_\mathrm{d} - \epsilon_\mathrm{a} = 0.37$, 0.36, 0.16 eV für Methanol, Wasser bzw. Acetylen bestimmt. Ein Vergleich dieser Ergebnisse mit Systemen wie Diethylether oder Ethylen auf Si(001) zeigt, dass die Konversion der hier untersuchten Moleküle vergleichsweise wenig Aktivierungsenergie benötigt und auf kurzen Zeitskalen verläuft. Für Methanol und Wasser wurde dies auf einen Protontransfer zurückgeführt, der im Vergleich zu der Dissoziation einer O-C-Bindung im Falle der Adsorption von Ether-Molekülen leichter abläuft. Im Fall von Acetylen wurde die schnelle Konversion mit der schwachen Bindungsenergie der Moleküle im Zwischenzustand erklärt, welcher auf der geringern Dreizentrenbindung zwischen den π-Elektronen des Acetylenmoleküls und dem positiv geladenen $\mathrm{D_{down}}$-Orbital eines Siliziumdimers basiert, sowie der generell höher Reaktivität der Dreifachbindung erklärt. Aufbauend auf den Unterschieden der untersuchten Systeme bezüglich ihrer Adsorptionskinetik wurden Experimente zur Untersuchung der Adsorptionsdynamik durchgeführt, wobei insbesondere die Abhängigkeit des Anfangshaftkoeffizienten s_0 von der kinetischen Energie der adsorbierenden Moleküle, E_kin, bestimmt wurde. Dabei zeigte sich, dass der ausschlaggebende Faktor, der die Adsorptionsdynamik beeinflusst, die Art des Zwischenzustands ist, unabhängig von den Details der adsorbierten Moleküle oder ihrer möglichen weiteren Reaktionen, beispielsweise der Konversion in einen Endzustand. Die unterschiedliche Abhängigkeit von s_0 bezüglich E_kin bietet die Möglichkeit zur gezielten Kontrolle der Reaktionen bezüglich der Adsorption in den Zwischenzustand.

Der zweite Teil der Arbeit umfasst Experimente zur anschließenden Manipulation

der Adsorbate nach der Konversion vom Zwischen- in einen Endzustand. Das System Diethylether auf Si(001) wurde dabei als Beispielsystem untersucht. Im Endzustand können die adsorbierten Moleküle in zwei unterschiedlichen Konfigurationen vorliegen. Beiderseitige Umwandlungen zwischen diesen zwei Konfigurationen konnten mittels Rastertunnelmikroskopie beobachtet und charakterisiert werden. Die Konversion zwischen den beiden Subzuständen kann dabei auf ein thermisch aktiviertes Hüpfen des Alkyl-Fragments des gespaltenen Diethylether-Moleküls auf einem einzelnen Dimer zurückgeführt werden. Die relative Hüpfrate zeigt eine starke Abhängigkeit von der Tunnelspannung, bleibt jedoch unter Variation des Tunnelstroms konstant. Diese Beobachtung lässt sich mit der Verringerung der Energiebarriere der Konversion durch eine Depolarisation der C-Si-Bindung durch das elektrische Feld der negativ geladenen STM-Spitze erklären. Der Energiebeitrag des Feldes wurde auf mindestens 0.3 eV bestimmt, was gut mit der Stärke des elektrischen Feldes zwischen Spitze und Probe im Einklang steht.

Table of Contents

Chapter 1

Introduction

Semiconductor materials are the basis of the nowadays technology. Microelectronic devices such as memory chips used in computers and cell phones, photosensor, biological sensors, and photovoltaic cells are all examples where our everyday life and the continuously growing technology of semiconductor-based electronics are interconnected. Consequently, silicon and its compounds have attracted much interest not only with respect to bulk properties but also with respect to the surface and its functionalization by adsorbing organic molecules with various functional groups. The latter has been an active area of research in the last decades [1–6]. The research in this field was driven by the goal to fabricate novel nanostructured materials with tailored properties and to increase the functionality of semiconductor surfaces.

Although the research in the field of semiconductor functionalization is not restricted to a specific silicon surface, Si(001) has attracted most attention for multiple reasons: first, most of silicon-based integrated circuits are built on this surface. Second, despite its simple reconstruction, there is a wealth of different reaction schemes, which can be seen in analogy to organic chemistry. For this reason, the reactivity of a wide variety of organic molecules on Si(001) has been studied and investigated in detail either using experimental [9–17] or theoretical methods [18–21] or both combined [22–25]. The main focus of this research is to understand the adsorption pathway of the studied molecules from the gas phase into the kinetically stable final state, and to use this knowledge as a tool to achieve more control over such reactions. The adsorption -for most cases- was found to proceed via an intermediate state [26–28]. The chemical bonding of the intermediate and its binding energy depend on the chemical configuration of the molecule and the respective functional group. If a molecule converts to the final state, its adsorption configuration involves covalent bonds regardless if the conversion is dissociative or not [29–33]. This conversion from the intermediate into the final state has been a subject of intense research [34–39].

In this work, two different parts of the potential energy curve have been investigated in detail, i.e., the adsorption dynamics into the intermediate as well as the possibility to induce changes in the finale state when several final configurations are possible. A complete adsorption pathway is illustrated by the three dimensional potential energy curve (3D PES) in Fig. 1.1 [7, 40, 41] and the processes investigated in

this thesis are highlighted in red in this PES.

The 3D PES emphasizes the concept of a decoupling between adsorption into the intermediate and the final state, which was proposed based on the investigation of the adsorption dynamics of tetrahydrofuran (THF) and trimethylamine (TMA) on Si(001) [42]. According to this concept, the gas/surface adsorption dynamics are mainly determined by the intermediate state regardless how the reaction further proceeds. The concept of the decoupling has motivated further research on systems with similar adsorption pathway but different adsorption kinetics. In this work, we will show by using molecular beam techniques that for methanol/Si(001) and water/Si(001) the energy barrier for the conversion from the intermediate into the final state is considerably low (articles I and III), especially when compared to the adsorption of

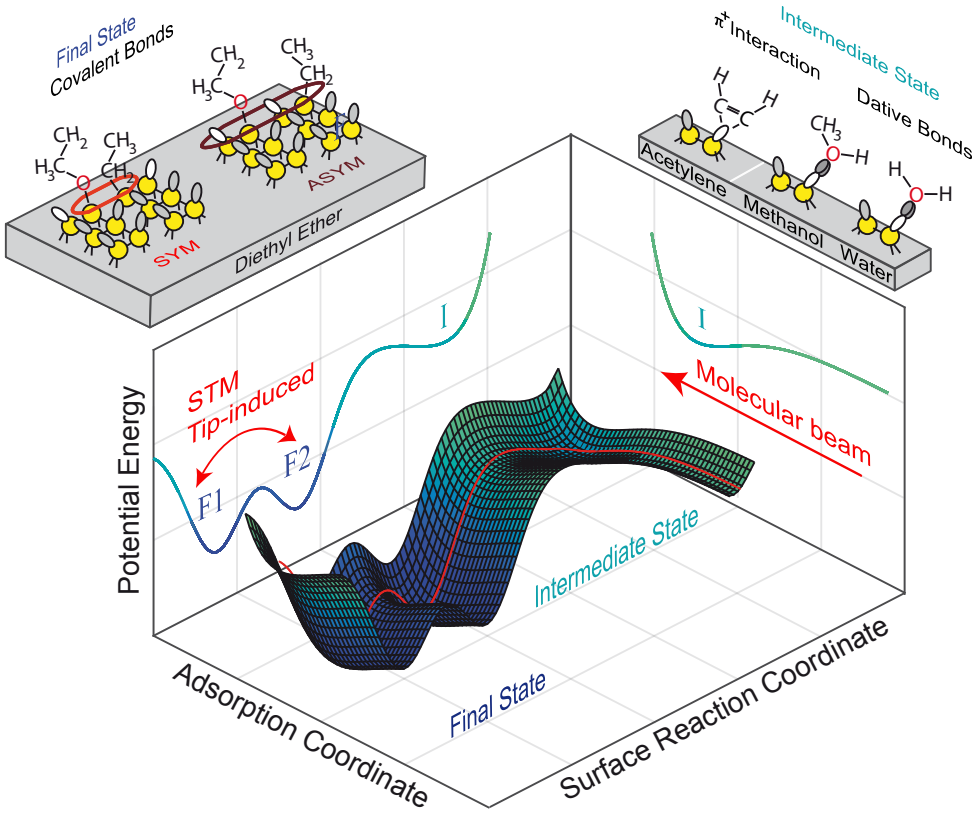

Fig. 1.1: Pseudo 3D representation of the potential energy surface for organic molecules on Si(001). In this representation, the reaction coordinates into the intermediate (adsorption coordinate) and from the intermediate into the final state are orthogonal, and thus largely decoupled [7, 8]. The adsorption from the gas phase into the intermediate state are studied using molecular beam techniques. The final state is separated in two sub-final-states in the case of diethyl ether molecule. In this work, the manipulation of the alkyl fragment of the cleaved ether molecule in the final state is possible with STM tip.

diethyl ether on Si(001) [42, 43]. One of the two major questions discussed in the framework of this thesis is then how such a fast conversion will affect the adsorption dynamics (article III), and if the decoupling applies even for such a kinetically unstable intermediate state. The second question is assigned to the study of molecules after the conversion into the final state. As the final state of many systems consists of a multiple adsorption configurations which are energetically very comparable, a further control of the adsorbate/substrate system in these states is of interest. In article IV, it is shown that such control is possible by the electric field in the tunneling junction of an STM setup, even in the case of covalently bonded final states on Si(001).

In the following, an overview over the applied experimental setups will be given in chapter 2 before these two main aspects of the thesis are discussed in section 3.1 and section 3.2.

Chapter 2

Experimental Setup

2.1 Molecular Beam Experiment

2.1.1 Beam Properties

A Molecular beam experiment [33, 44, 45] is used to study the adsorption dynamics of organic molecules on Si(001) [7, 8, 42]. This is accomplished by determining the sticking coefficient at different kinetic energies and surface temperatures. The molecular beam is generated by a supersonic expansion of the molecules from their reservoir to the sample chamber (base pressure 2×10^{-11} mbar) through a nozzle of 100 µm diameter.

The molecules impinge at normal incidence on the sample surface with a controlled

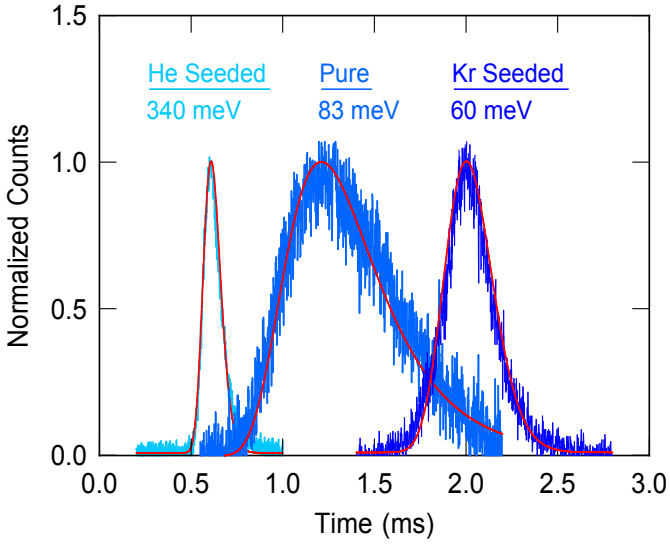

Fig. 2.1: TOF Spectra of methanol molecules for the following three cases: pure beam, methanol seeded in helium beam and methanol seeded in krypton beam. Not only the velocity of the molecules changes by using a seeded beam, but also the velocity distribution $\Delta\nu/\nu_0$ due to the high total pressure in the nozzle.

kinetic energy, which depends on the difference of the pressure in the reservoir and the vacuum chamber and on the temperature of the nozzle. The increase in kinetic energy is proportional to the difference in the temperature before and after the expansion via $E_{\mathrm{kin}} = C_{\mathrm{P}} \times \Delta T$ [46]. Thus by heating the nozzle, the kinetic energy of the beam can be increased.

Another possibility to change the kinetic energy of the molecules in the beam is to apply the so called seeding beam technique, which is a process of mixing the studied molecules with an inert gas [47] of a different atomic mass to increase or decrease the kinetic energy of the expanding molecules. The mean kinetic energy as well as the energy distribution can be determined by applying time-of-flight measurements (TOF). In this method, the time the molecules spend to travel a known distance from a chopper to a quadruple mass spectrometer (QMS) is measured. The chopper chops the beam into multiple short pulses in order to determine the time of flight of the molecules and with this their velocity distribution by knowing the distance between the chopper and the QMS. By using the known mass of the molecules, the kinetic energy of the molecules and its distribution is determined [48]. An example of this measurement is shown in Fig. 2.1 for three different seeding experiments. A wider distribution of the TOF spectrum is obtained in the case of pure methanol. The width of the distribution depends on the pressure and the expansion temperature. By seeding the molecules either with helium (atomic mass m_{a}=4 u) or with krypton (m_{a}=84 u), the translational kinetic energy of the beam is increased or decreases respectively. In both cases, the velocity distribution is narrower when compared to the pure methanol beam due to the larger number of collisions during the expansion of the molecules from the nozzle given by the higher total pressure therein.

2.1.2 Sticking Coefficient Measurement

The sticking coefficient is measured by applying the classical method of King and Wells [49]. In this method, a nonreactive shutter is used to block the molecules in front of the sample (Fig. 2.2 (a), inset). When the shutter is opened at t=0, the QMS signal drops due to the adsorption of the molecules on the sample surface. The initial sticking coefficient is proportional to the initial drop in the signal. In the case of methanol and water beams, the initial sticking coefficient directly based on this drop is underestimated. This is due to the response of the chamber characterized by the so-called chamber response function $f(\mathrm{t})$ [7, 42, 50]: When the beam is on, an equilibrium between molecules adsorbed on the chamber walls and the gas phase is established. When the shutter is opened, a part of the molecules desorbing from the chamber walls contribute to the QMS signal. This leads to an apparent initial drop in the signal smaller than the actual one caused by the adsorption on the surface only. For this reason, $f(\mathrm{t})$ has to be taken into account in order to get the actual values of the initial sticking coefficient. $f(\mathrm{t})$ was recorded by shutting off the beam without

opening the shutter and recording the gradual decrease in the QMS signal (Fig. 2.2 (a), black curve). By subtracting the background and normalizing adsorption curves and then inverting them, the apparent sticking probability as a function of time is obtained (Fig. 2.2 (b), blue curve). After considering the inverted f(t)-function (black curve), the actual sticking coefficient is determined by fitting a tanh-function to the final data (red dashed curve).

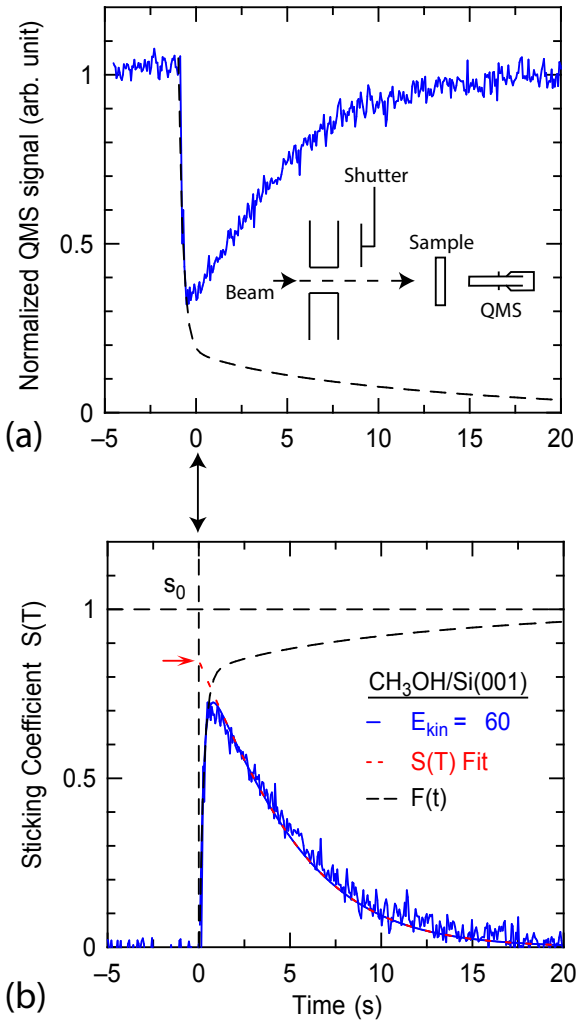

Fig. 2.2: Adsorption of methanol on Si(001) measured by means of King and Wells method. In (a), the curve shows the drop in the QMS signal after the shutter is opened at $t = 0$. The black curve is the chamber response function f(t). In (b), the raw adsorption curve is normalized and inverted (blue solid curve). The dashed red curve is the fit of the data taking into account the compensation of the f(t). The red arrow indicates the value of the initial sticking coefficient s_0 after the compensation.

2.2 Variable Temperature Scanning Tunneling Microscopy

2.2.1 Principle

Scanning tunneling microscopy (STM) is an indispensable tool for studying structure and electronic configuration of surfaces with atomic resolution [51, 52]. This revolutionary experimental instrument was developed based on the concept of quantum tunneling, which is a purely quantum mechanical phenomenon with no equivalent in classical physics. The working principle of STM is described as following: If we place a metal tip near to a surface to be scanned, an electron in the tip can tunnel into the sample (or vice versa) even without a direct contact. If the electron has an energy E and encounters a potential barrier $U(z)$ in the gap between the tip and the sample (Fig. 2.3), the spatial distribution of the wave function $\psi(z)$ of the electron is given by Schrodinger equation:

$$\frac{-\hbar^2}{2m}\frac{d^2}{dz^2}\psi(z) + U(z)\psi(z) = E\psi(z) \tag{2.1}$$

The solution of (2.1) in the region where $U(z) > E$ is given by $\psi(z) = \psi(0)e^{-\kappa z}$. This indicates that the tunneling probability vanishes rapidly with the barrier width z, which is in this case the distance (if the tip is at negative bias).

According to Bardeen [54], the tunneling current is a convolution of the local density of states of the tip ρ_{t} and the local density of states of the sample ρ_{s}. This

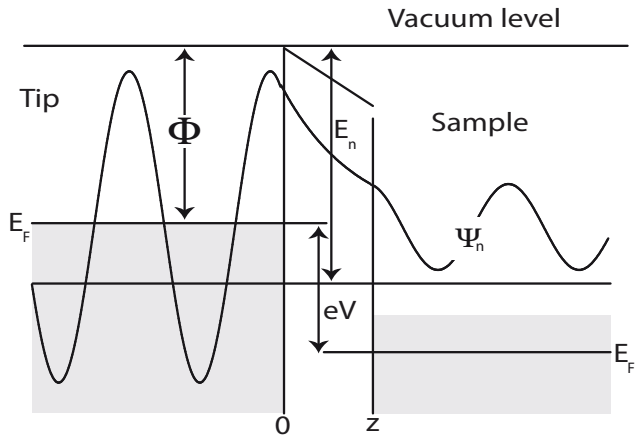

Fig. 2.3: Illustration of one-dimensional tunneling junction (from [53]): the tip state ψ_{n} has a nonvanishing probability at the sample surface. This probability decreases exponentially with the width of the tunneling junction.

convolution is expressed by the following integral:

$$I = \frac{4\pi e}{\hbar} \int_0^{eV} \rho_t(E_F - eV + \epsilon)\rho_s(E_F + \epsilon)|M|^2 d\epsilon \tag{2.2}$$

with the tunneling matrix element M, which is often assumed to be constant in the case of small tunneling bias. Bardeen equation (2.2) summarizes the factors determining the tunneling current in the case of vanishing thermal excitation and in the case of metallic sample surface. Additional considerations have to be taken into account in the case of a metal/semiconductor junction. The tunneling from the electronic states of the tip to the electronic states of the semiconductor surface and vise versa is illustrated in Fig. 2.4 for the two different tunneling polarities. Due to the exponential dependence of the tunneling probability on the height of the barrier, the highest occupied states contribute most to the tunneling current in Fig. 2.4 (a), and the unoccupied states at E_f+eV contribute most to the tunneling current in Fig. 2.4 (b).

A very important quantity for the context of the thesis is the so-called transmission coefficient T given by:

$$T \equiv \frac{I(z)}{I(0)} = e^{-2\kappa z} \tag{2.3}$$

where $\kappa = \frac{\sqrt{2m\phi}}{\hbar}$ is the decay constant. The transmission coefficient T describes the strong decreasing of the tunneling current $I(z)$ with increasing z. At typical condition, a very small change in z of 1 Å results in an increase of I by one order of magnitude [53]. This means that the tunneling is spatially localized under the top-most atom of the tip. This is the origin of the atomic resolution in STM. The effect of tunneling electrons and the electric field in the tunneling junction on possible manipulation of adsorbates on surfaces is discussed in the next section.

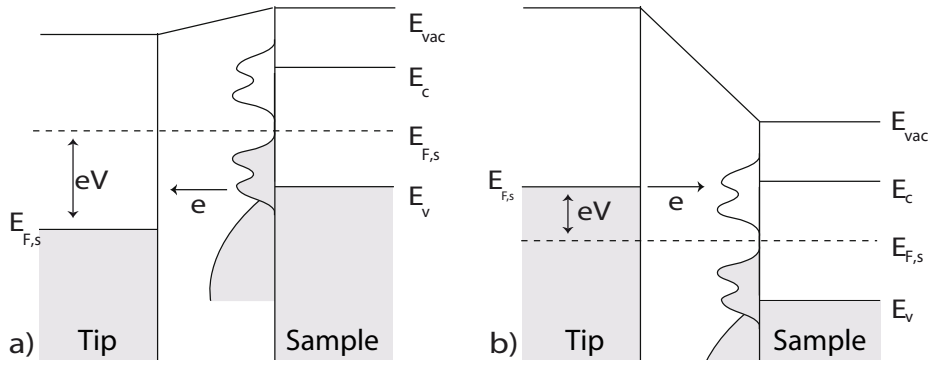

Fig. 2.4: Illustration of metal-semiconductor tunneling junction for negative (a) and positive (b) sample bias (from [55, 56]). The tunneling current is dependent on the density of states between E_f-eV and and E_f.

2.2.2 Manipulation of Adsorbates on Surfaces with the STM Tip

Beside the usage of STM as an imaging instrument, the STM tip has been widely used as a nanometric tool to manipulate atoms and molecules on surfaces [57–65]. The mechanisms by which a tip can manipulate adsorbates on surfaces are diverse. They involve direct interatomic forces between the tip and adsorbates [63, 66], and electronic or vibrational excitation of the manipulated adsorbates [59, 61, 67]. The latter results from the interaction between tunneling electrons and adsorbates: tunneling electrons transfer part of their energy during tunneling causing multiple vibrational excitations in the adsorbate, or the tunneling electrons can directly electronically ionize or excite the adsorbate (Fig. 2.5). In both cases, the dependence of the manipulation rate on the tunneling current follows a power law $R \propto I^n$ depending on the number of tunneling electrons n involved in the process [68–70].

Another important manipulation mechanism of adsorbates on surfaces is the electric field in a tunneling junction [71–74]: By applying a bias voltage between tip and sample, not only a tunneling current occurs, but also a large (inhomogeneous) electric field in the tunneling junction is established. This field depends on the distance between the tip and the sample, on the bias voltage, and on the shape of the tip [73, 75, 76]. As mentioned in 2.2.1, the tunneling current depends exponential on the distance between the tip and the sample. Therefore, only a substantial increase in the tunneling current can result in a considerable change in the electric field at a given

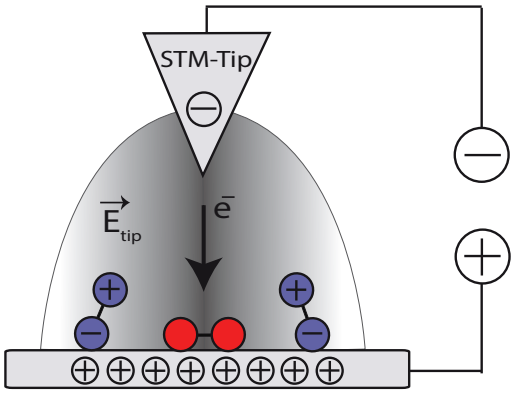

Fig. 2.5: Sketch of an inhomogeneous electric filed under an STM tip. The electric field is not restricted under the top-most atom of the tip, but the tunneling current is. In contrast to electronic excitation (red-colored molecules), the molecules in the case of field induced manipulation is not restricted to a location directly under the apex of the tip (blue-colored molecules). The electric field depolarizes or increases the polarization of an adsorbate depending on the polarity of the tunneling junction and the initial polarization of the adsorbate/substrate system.

tunneling bias. In contrast, increasing the bias voltage directly results in a substantial increase of the electric field.

In addition, manipulation induced by tunneling electrons is localized under the top-most atom of the tip. In contrast, field induced manipulation is not localized by necessity as the manipulated adsorbate has only to be in the effective area of the tip electric field (Fig. 2.5).

Chapter 3

Results and Discussion

3.1 Influence of Intermediate State on Reaction Dynamics and Kinetics

In this section, first the adsorption kinetics and energetics of methanol, water, and acetylene on Si(001) are investigated and compared to the adsorption of diethyl ether on Si(001) [43]. Major differences are observed for the compared systems. The influence of these differences in the energetics on the adsorption dynamics is investigated in the second part. The results described in this chapter are explained in detail in articles I and III.

3.1.1 Reaction Kinetics

The energetics of the adsorption pathway of methanol and water on Si(001) were determined by measuring the initial sticking coefficient as a function of surface temperature $s_0(T_s)$ (Fig. 3.1, dark and light blue respectively). For comparison, $s_0(T_s)$ of acetylene was measured as well (Fig. 3.1, light brown data). Acetylene has a strong triple carbon carbon bond as a functional group, in contrast to the single oxygen heteroatom in methanol and water. For the three compared molecules, s_0 has a similar qualitative dependence on T_s: s_0 remains constant up to a threshold surface temperature ($T_{th} \approx 450$ K for water and methanol, ≈ 220 K for acetylene). At temperatures higher than T_{th}, s_0 drops continuously approaching 0.2 at high T_s. Qualitatively, such a behavior is characteristic for adsorption of organic molecules on semiconductor surfaces and is explained in terms of adsorption via an intermediate state [7, 8, 22, 43, 77, 78]: Incident molecules adsorb first in the intermediate state with a binding energy of ϵ_d, which equals the desorption barrier in the case of a non-activated adsorption pathway (Fig. 3.3). At low surface temperature, the molecules either reside in the intermediate state for a period of time longer than the time scale of the experiment, or they convert into the covalently bonded final state by overcoming the energy barrier ϵ_a. At increased surface temperature, however, the number of the desorption events from the intermediate state to the gas phase relative to the number

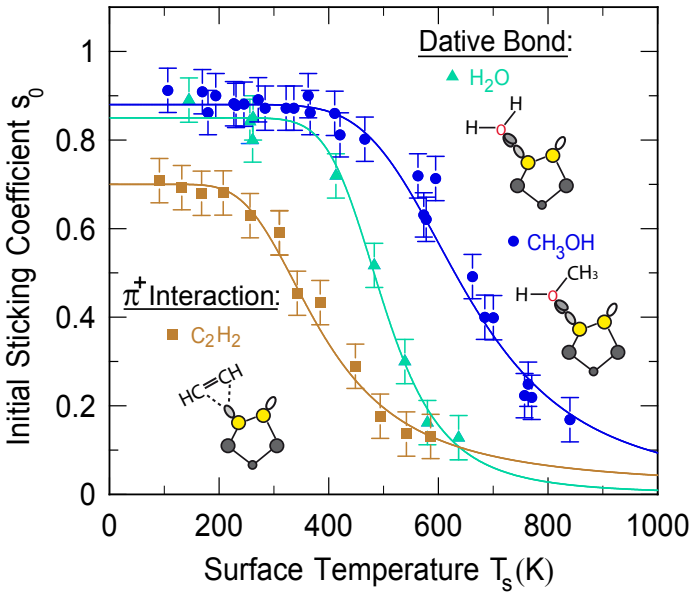

Fig. 3.1: Initial sticking coefficients s_0 of methanol and water on Si(001) as a function of surface temperature T_s. For comparison, the dependence of s_0 on (T_s) of acetylene on Si(001) is shown. The type of the intermediate bonding for each molecule is sketched.

of the molecules which convert from the intermediate into the final state, increases and results in the continuous drop of s_0.

The competition between the two processes at increased surface temperature can be described quantitatively using the Kisliuk model [79]. The initial sticking coefficient according to this model is given by

$$s_0 = s_p \cdot \frac{k_a}{k_a + k_d} \quad \text{with} \quad k_i = \nu_i . e^{\frac{-\epsilon_i}{k_B T}} \tag{3.1}$$

where s_0 is the probability that the incoming molecule is adsorbed in the intermediate state ($s_0 \approx 0.9$ for water and methanol, and 0.7 for acetylene), k_a and k_d are the rates of the thermally induced conversion into the final state and the desorption back into the gas phase, respectively; ν_i and ϵ_i are the corresponding pre-exponential factor and the energy barrier, respectively. Eq. 3.1 can be rewritten as following:

$$\ln\left(\frac{1}{s_0/s_{0,\max}} - 1\right) = \ln\left(\frac{\nu_d}{\nu_a}\right) - \left(\frac{\varepsilon_d - \varepsilon_a}{k_B T_s}\right) \tag{3.2}$$

The data of Fig. 3.1 are shown according to Eq. 3.2 in Fig. 3.2. The observed linear dependence indicates the applicability of the model. The quantity $\epsilon_d - \epsilon_a$, i.e. the energy difference between the desorption barrier ϵ_d and the conversion barrier ϵ_a is deduced from the slope of data in Fig. 3.2.

Almost the same value of $\epsilon_d - \epsilon_a$ is obtained for water and methanol (0.36 and

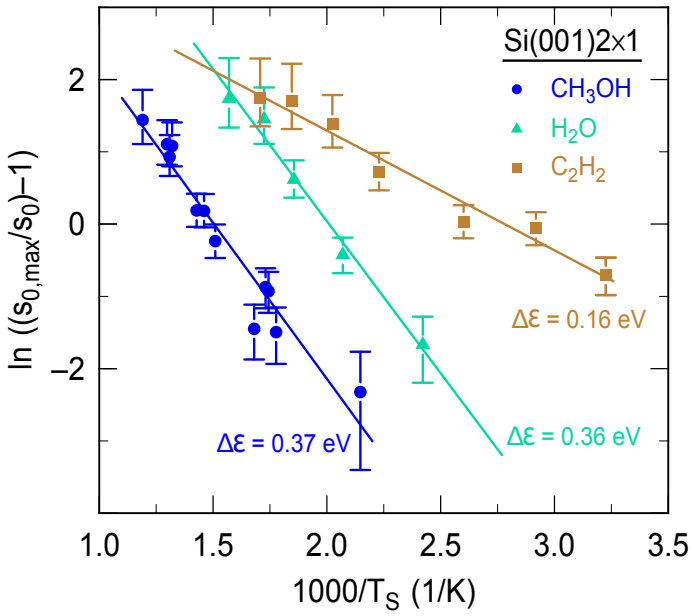

Fig. 3.2: Data of Fig. 3.1 plotted according to the Kisliuk model (Eq. 3.1). Only the range of the two competing processes was included in the fitting: from $T \approx 450$ to 1000 K for water and methanol and from $T \approx 200$ to 600 K for acetylene. The resulting values of energy difference $\epsilon_d - \epsilon_a$ of methanol and water are comparable (0.37 eV and 0.36 eV, respectively), but they differ considerably from that of acetylene (0.16 eV).

0.37 eV, respectively). The obtained energy difference is large, especially if it is compared to molecules with similar configuration such as diethyl ether, which reacts via its oxygen heteroatom as well. The key parameters of the potential energy curve of diethyl ether on Si(001) was determined experimentally (Fig. 3.3) [43]. The value of the energy difference in this case is $\epsilon_d - \epsilon_a = 0.24$ eV, and the conversion barrier was determined by means of second harmonic generation experiment SHG as $\epsilon_a = 0.38$ eV [43]. Therefore, the binding energy of the intermediate state was deduced as $\epsilon_d = 0.62$ eV. Such a stable intermediate, however, is neither expected for methanol nor for water because of the missing positive inductive effect of the hydrogen oxygen bond in these both molecules in comparison to the positive inductive effect of the alkyl chain in the case of diethyl ether. The missing positive inductive effect destabilizes the dative bond and leads to weaker binding of the methanol and water molecules in the intermediate state. For this reason, the maximum conversion barrier for methanol and water is estimated to be $\epsilon_{a,max} \approx 0.6$ - 0.4 eV = 0.2 eV. This lower conversion barrier is attributed to a different underlying conversion process involving a proton transfer from the datively bonded molecule to the silicon atom either of the same dimer or the following one on the same row [18, 80–82].

This process is associated with a lower energy barrier [83] if compared to the cleavage of the oxygen-carbon bond during the conversion of the diethyl ether from

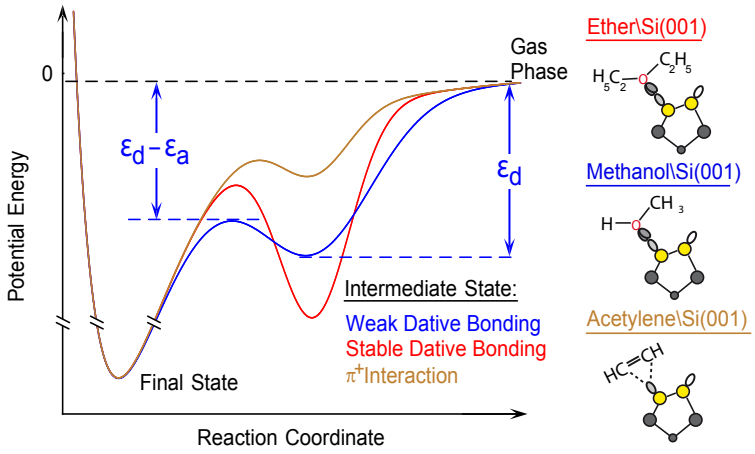

Fig. 3.3: A comparison between the potential energy curve of methanol and water (blue) diethyl ether (red) (from [43]), and acetylene (light brown) on Si(001). The low energy barrier in the case of methanol and water in comparison to diethyl ether explains the fast conversion from the intermediate into the final state (proton-transfer reaction) (from [80]). The low barrier ϵ_a for acetylene is attributed to the weak bonding of the intermediate state (π interaction).

the intermediate to the final state [29, 43]. For acetylene on Si(001), a considerably lower value for the energy difference is obtained ($\epsilon_d - \epsilon_a \approx 0.16$ eV, Fig. 3.3). For a quantitative comparison, we need to estimate the binding energy of the intermediate state of acetylene as well. The binding of the intermediate in this case is expected to be considerably weaker even in comparison with alcohols because it involves a thee center bond between the the π-electrons of the molecule and the positively charged D_{down} state of the silicon dimer. If we take ϵ_a for acetylene to be between the binding energy of alcohols (see above) [8, 80] and ethylene (0.3 eV) but closer to that of ethylene [78, 84], a conversion barrier of $\epsilon_d \approx 0.2$ eV is deduced [85]. The conversion barrier ϵ_a, according to our quantification, is considerably reduced if compared to that of diethyl ether. Our quantification of ϵ_d for acetylene is supported by some theoretical studies as well [86, 87]. An average value of $\epsilon_d \approx 0.15$ eV was found according to these studies, which matches our quantification well. The resulting values of ϵ_a and ϵ_d according to our quantification are summarized in Tab. 3.1.

This comparison indicates that the conversion from the intermediate into the final state for the three studied molecules is very fast in comparison to the conversion of diethyl ether, so that experiments such as scanning tunneling microscopy (STM) and X-ray photoelectron spectroscopy (XPS) are not fast enough to detect the intermediate state in the case of the three molecules at low temperatures [8, 80]. A qualitative overview of the potential energy curves (PES) of the discussed cases is shown in Fig. 3.3.

Tab. 3.1: Binding energy ϵ_d and the conversion barrier ϵ_a as obtained for the three studied molecules. The data of diethyl ether/Si(001) are listed for comparison (from [43]).

Barrier \ Molecule	Ether	Water	Methanol	Acetylene
$\epsilon_d - \epsilon_a$ (eV)	0.3	0.4	0.4	≈ 0.2
ϵ_d (eV)	0.6	0.6	0.6	≈ 0.3
ϵ_a (eV)	0.3	0.2	0.2	0.1

3.1.2 Reaction Dynamics

The adsorption dynamics of methanol and water on Si(001) were studied by varying the kinetic energy E_{kin} of the impinging molecules and measuring the initial sticking coefficient s_0 as a function of E_{kin}. The results are shown in Fig. 3.4 for methanol and water in blue and green, respectively. The dependence of s_0 on E_{kin} is characteristic for a nonactivated adsorption channel as s_0 decreases continuously with E_{kin}. The molecules are more easily reflected from the repulsive part of the potential energy curve (PES) at increased E_{kin} as they have to lose more energy for being trapped. Qualitatively, this compares well with other studied molecules such as THF and ethylene (Fig. 3.4, red and brown lines respectively [42, 78]).

Methanol, water, and ether differ in molecular mass and the number of the atoms, which determines the internal degree of freedom (Tab. 3.2). Moreover, the conversion of methanol and water from the intermediate into the final state proceeds considerably faster in comparison to THF as we found in the previous section. Nevertheless, the reaction dynamics that is $s_0(E_{kin})$, obtained for the three molecules are very similar. Even when the adsorption is overall activated as in the case of of TMA/Si(001), a similar dependence of s_0 on E_{kin} is obtained (Fig. 3.4, gray dotted line) [7]. The common feature between these molecules is that their adsorption proceeds via a datively bonded intermediate state. For comparison, we take an example with different binding in the intermediate such a ethylene, which has comparable mass and number of atoms as methanol, but adsorbs via an intermediate state involving a weak π interaction. For ethylene, a much faster drop in s_0 is observed at increased E_{kin} in comparison to other cases. This is taken as a further indication that the decisive factor in the adsorption dynamics is the nature of the intermediate state. The effects of molecular size, the number of its atoms, or any further possible conversion into the final state are of minor importance.

Since the reaction dynamics is completely governed by the intermediate state, regardless how fast the reaction further proceeds, intermediate and final states are seen to be decoupled. To illustrated this, the 2D potential energy curve with one axis denoting the potential energy and the second one denoting the reaction coordinate is decomposed into a 3D potential energy surface [7, 40, 41]. One axis denotes the

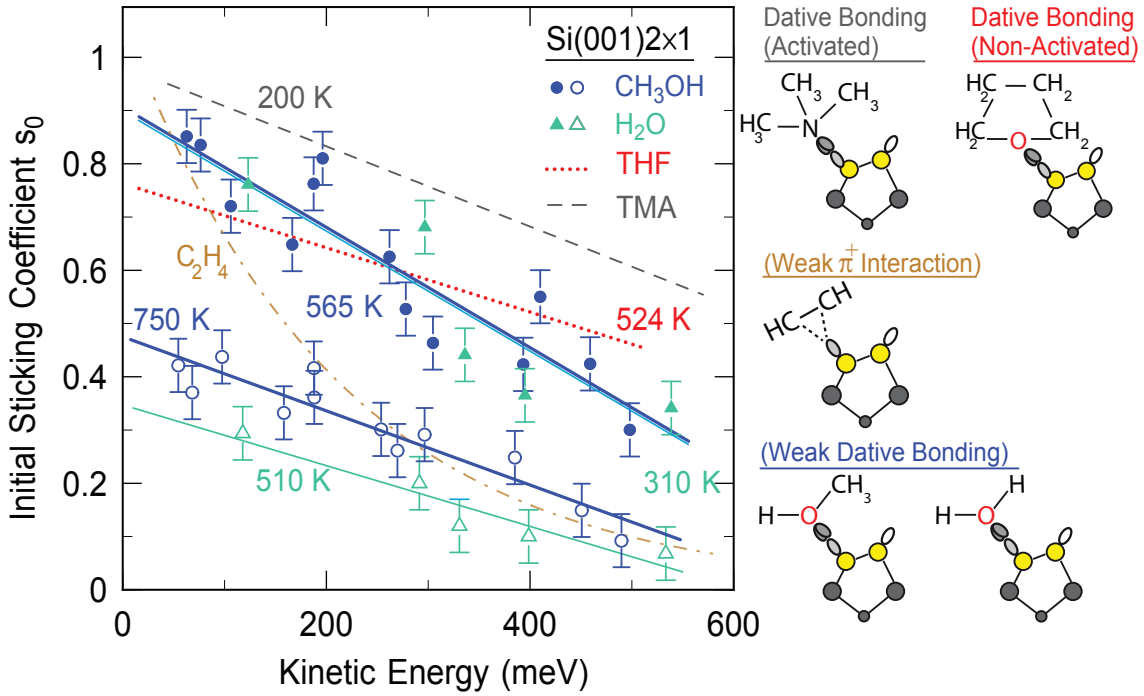

Fig. 3.4: Initial sticking coefficients s_0 as a function of kinetic energy E_{kin} for methanol (dots) and water (triangles) on Si(001) at surface temperatures 565 K and 510 K respectively. The results of THF (dotted red line) , TMA (gray dashed line), and ethylene (brown dashdotted line) are also shown at 524 K, 200 K, and 150 K respectively (from [42, 78]). The corresponding intermediate for each molecule is sketched on right.

binding of the different adsorption stages (potential energy). The second axis reflects the adsorption coordinate, i.e., the adsorption into the intermediate state. The third axis then reflects any further possible reaction (i.e., a possible conversion into the final state). This is illustrated schematically in Fig. 3.5. If the latter two coordinates are mainly decoupled, they are orthogonal with respect to each other in this representation. At high beam energy, the impinging molecules thus are not reflected from the repulsive part of the final state as it is oversimplified by the 2D PES, but rather from the repulsive part of the decoupled intermediate state. The nature of any further

Tab. 3.2: A comparison of the molecular properties of the studied molecules. The data of diethyl ether, TMA, and ethylene are taken from [42, 78].

Property \ Molecule	Et_2O	Water	Methanol	Acetylene	TMA
Number of Atoms	13	3	6	4	13
Molecular Mass	72	18	32	26	59
ϵ_a (eV)	0.3	< 0.2	< 0.2	≈ 0.1	$> \epsilon_d$

reaction after the adsorption in the intermediate and how fast it proceeds, is largely irrelevant with respect to the adsorption dynamics.

The different dependence of s_0 on E_{kin} for different molecules (Fig. 3.4) and the proposed decoupling of the adsorption coordinates (Fig. 3.5) can be envisioned as a possibility to have more control on the adsorption of organic molecules on Si(001) [85, 88]. For example, acetylene and alcohol adsorb differently at increased kinetic energy as they have considerably different s_0 at increased E_{kin}. Consequently, the final product of the adsorption of larger molecules with multiple functional groups (e.g., a C-C triple bond and oxygen heteroatom) can be systematically controlled.

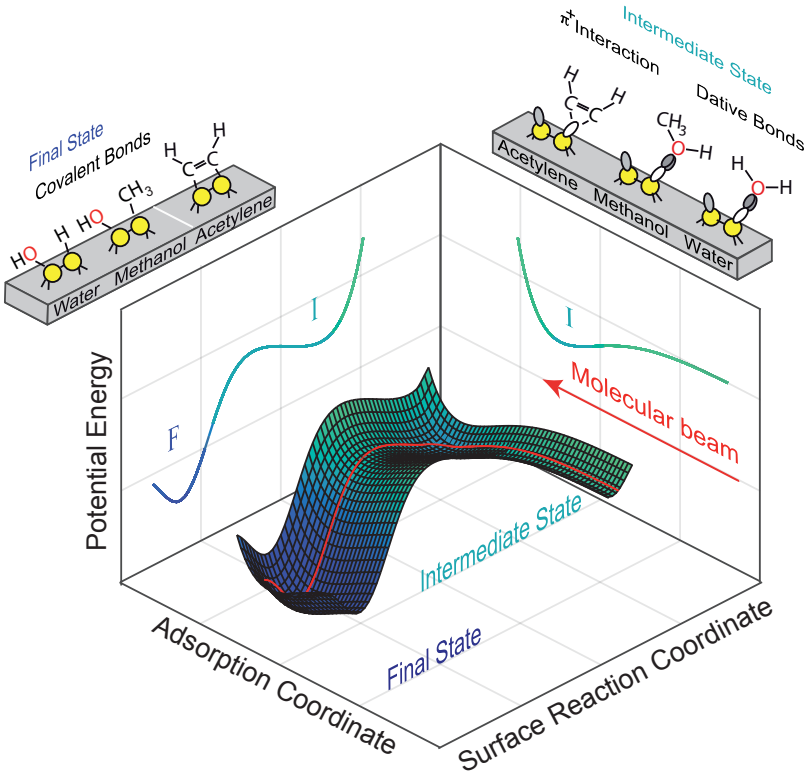

Fig. 3.5: 3D model potential for the adsorption of organic molecules on Si(001) to illustrate the decoupling of the reaction coordinates. The dynamics are largely determined by the existence of an intermediate state and the adsorption into this intermediate state, i.e., the movement of an adsorbate along the adsorption coordinate., and is not affect by the nature of any possible further reaction. The further reaction along the surface reaction coordinate has little effect on the dynamics.

3.2 Manipulation of Adsorbates in the Final State

The possible reactivity of adsorbates on Si(001) after conversion from the intermediate into the final state is discussed in this section. We take diethyl ether $(C_2H_5)_2O$ on Si(001) as an example for this investigation, which follows an adsorption pathway from a datively bonded intermediate into a covalently bonded final state; this final state consists of two covalently bonded configurations. The manipulation of the molecule in these states, i.e., controlled switching between these states, is discussed. The experimental setup used for this experiment is a scanning tunneling microscope used at variable temperature. The results of this section are discussed in detail in article IV.

3.2.1 Multiple Final States: Diethyl Ether on Si(001)

Diethyl ether follows the typical adsorption pathway of organic molecules on Si(001) via an intermediate state [32, 43]. The conversion into the covalently bonded final state is concomitant with a cleavage of the O-C bond at increased surface temperature (Fig. 3.6).

The final state in this case as in many other cases [31, 89, 90] consists of two different adsorption configurations (Fig. 3.6). After the dissociation, the two resulting

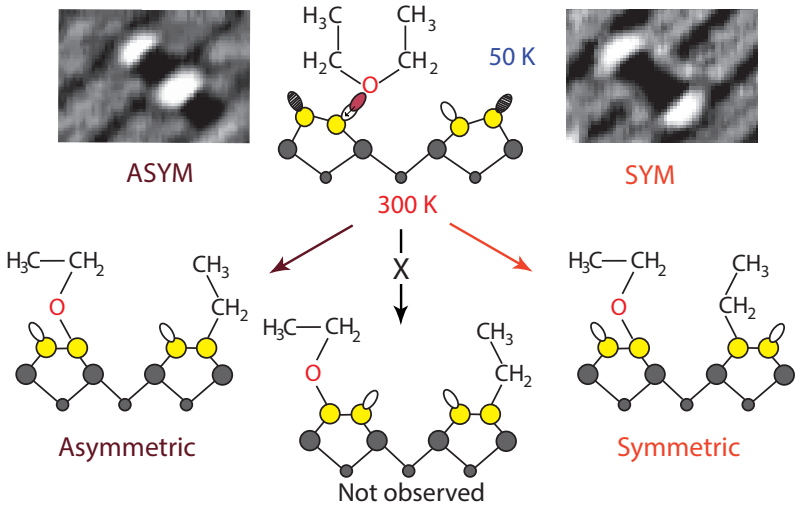

Fig. 3.6: Dissociation pathways of diethyl ether on Si(001). At 50 K, the oxygen hetroatom binds datively to a D_{down} state of a silicon dimer. At 300 K, diethyl ether dissociates into two adsorption configurations: symmetric (SYM, right) and asymmetric (ASYM, left). The oxygen hetroatom remains bonded to the same silicon atom after the dissociation. A configuration with the two molecular fragments being bonded to the two outer Si atoms of two neighboring silicon dimers is thus not observed.

molecular fragments -OCH_2CH_3 and -CH_2CH_3 form two covalent bonds with two neighboring dimers either symmetrically or asymmetrically with respect to the dimer rows. The two resulting adsorption configurations are well resolved using STM at room temperature (Fig. 3.6). They can be identified from the apparent pairs of bright spots, which are attributed to the unsaturated dangling bonds neighbored by two black spots attributed to the adsorbed molecular fragments. By scanning the same area on the surface consecutively, conversion events from the symmetric adsorption configuration to the asymmetric one and vice versa are observed (Fig. 3.7). The hopping events were observed only with positive sample bias, therefore they are interpreted as tip-induced hopping of one of the two molecular fragments. This indicates that a further manipulation of the adsorbates even in the covalently bonded final state is possible. A third configuration with the two molecular fragments being bonded to the outer Si atoms of two neighboring silicon dimers was not observed. We thus conclude that the -OCH_2CH_3 fragment with the oxygen atom remains bonded to the same Si atom it was bound to prior to molecular dissociation and the hopping fragment is the -CH_2CH_3 fragment.

This hopping fragment can move in both directions, as we observe conversions from symmetric to the asymmetric configurations and vice versa. In Fig. 3.7 (b), it is shown that two images are typically enough to characterize the conversion events, as we observe a certain adsorption configuration in the first image, and a new configuration in the following one. For $\approx 5\%$ of the hopping events, however, three images are necessary to characterize a hopping event (split feature, blue frame of Fig. 3.7 (b)). The hopping event in this case occurs when the tip was at least in a scan line which goes across the moving fragment. The first type of hopping indicates that the tip doesn't have to be in a restricted position close to the molecule to induce a hopping event, and the electrons are not necessarily injected in the empty states of a molecule during the hopping process. The fragment has only to be in the effective area of the tunneling junction to move. Scanning 1240 molecules with negative sample bias at 300 K resulted in zero hopping events. No hopping events were observed with positive sample bias and 50 K. The hopping events were exclusively observed with positive sample bias at 300 K. In order to find out the excitation mechanism of the alkyl fragment, we will look next at the hopping rate R as a function to the tunneling current and bias voltage.

3.2.2 Field-induced Hopping of an Alkyl group on Si(001)

At 300 K and positive sample bias, the dependence of R on the bias voltage and the tunneling current is obtained in order to find out the underlying excitation mechanism. In Fig. 3.8, the dependence of R on I and V is shown. The hopping rate R exhibits a vanishing dependence on the tunneling current at constant voltage and scan speed.

The number of the electrons tunneling through the molecular fragment increases by a factor of 15, the hopping rate R nevertheless fluctuates around a constant value determined by the applied voltage. For this reason, we exclude a process driven by the tunneling electrons which could induce direct, electronic or vibrational excitations of the adsorbate, as this would result in a linear or polynomial dependence of the R on I [59, 67–69, 91]. This is our first indication of an electric field driven hopping process. By varying the tunneling current, the distance d between the tip and the sample decreases in order to increase the tunneling probability. This decrease is, however, negligible if we consider the exponential dependence of the current on the distance. For this reason, the electric field under the tip is considered to be constant in the range of the applied tunneling current. In order to back up our assumption, we take into account that the hopping events are not only induced when the electrons are tunneling in the empty states of the systems close to the hopping fragment as mentioned above. The fragment has only to be in the effective area of the electric field in order to move.

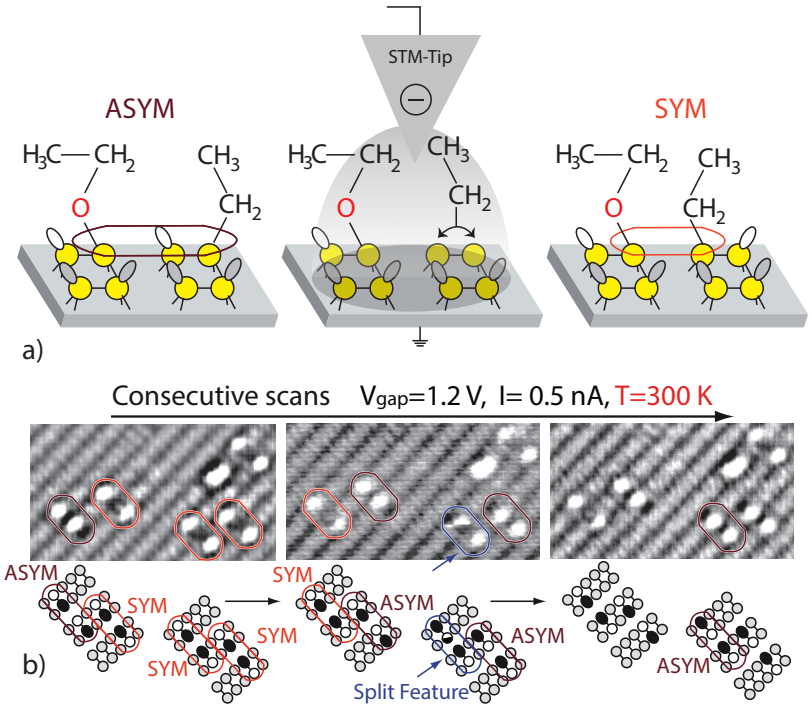

Fig. 3.7: (a) Illustration of the tip-induced conversion between the two adsorption configurations. The conversion results from the hopping of an alkyl fragment on top of one dimer. (b) Experimental observation of the tip-induced hopping by taking three consecutive images of the same area on the surface after adsorbing 0.15 ML of diethyl ether. Hopping events are indicated by a change from orange to brown frames and vice versa. The split feature is indicated by the blue arrow and frame.

The constant rate R with I excludes the possibility of excitation involving the injection of the electrons into surface states in the vicinity of a hopping fragment [92, 93] because such excitation mechanism would result in higher excitation probability at higher tunneling current. As it was repeatedly reported that the electric field under the tip depends on the shape of the tip and the contact potential [73, 75, 76, 94, 95], we attribute the fluctuation in R with I obvious in Fig. 3.8 to the usage of different tips during the experiment.

An additional indication of a field induced hopping is obtained from the dependence of the hopping rate on the bias voltage. First, the hopping rate increases nonlinearly with the applied voltage at constant tunneling current without a prominent threshold for the hopping process. Such a threshold would have indicated that electrons injected from the tip should have an energy higher than a threshold energy to induce the hopping events [96–99]. Hence, the increase of the rate R with the voltage V is attributed to the nonlinear increase of the area under the tip in which the field is strong enough to induce the observed hopping at increased voltage.

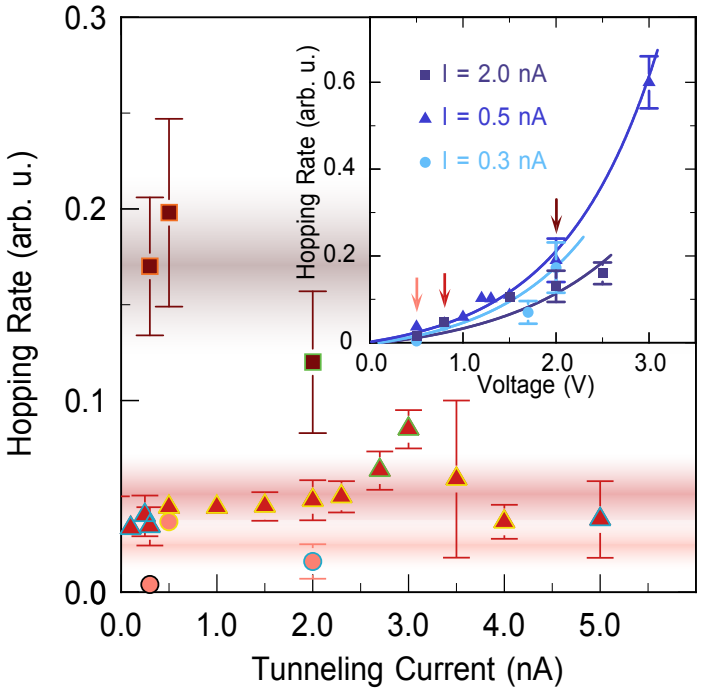

Fig. 3.8: The hopping rate R as a function of tunneling current (main panel) and bias voltage (inset). The three colored arrows in the inset indicate the bias voltages, at which the tunneling current was varied (0.5, 0.8 and 2.0 V). The symbols in the main panel of the same surrounding line were taken with the same tip.

3.2.3 Comparison with the Hopping of H on Si(001)

At 50 K, no hopping events were observed out of 240 scanned molecules; the observed hopping is thus concluded to be thermally activated. The electric field plays an assisting role, as it reduces the barrier, so that the hopping events can be observed on the time scale of the experiment at room temperature. The observation of hopping events exclusively with positive sample bias at room temperature indicates that the direction of the electric field couples to the polarity of the C-Si bond. The electric field depolarizes the bond leading to a reduced binding energy (Fig. 3.9, (c)). At room temperature and negative sample bias (positive tip, Fig. 3.9, (a)), the electric field is ineffective or it even increases the polarization of the bond. Since we scanned 1240 molecules with negative sample bias without observation of molecular hopping, we can estimate the minimum reduction of the thermal barrier by the electric field as following: The process is overall described by the following Arrhenius equation:

$$R'_{(300\ \mathrm{K},0.8\ \mathrm{V})} = A \times exp(-(\frac{\epsilon - \Delta\epsilon_\mathrm{f}}{k_\mathrm{B}T})) \tag{3.3}$$

Which indicates that the electric field reduces the thermal barrier ϵ with a contribution of $\Delta\epsilon_\mathrm{f}$ at 0.8 V. The rate R' denotes the hopping events per seconds in the presence of the electric field. It is determined by considering the scanning parameters (scan speed, frame size etc.), and the effective size of the electric field ($\phi \approx 6$ nm) as determined from the number of the split features with respect to the entire hopping events. The rate at 0.8 V is calculated as 10^{-4} s^{-1}. If we consider the 1240 scanned molecules at 300 K and -2.1 V without hopping to be the upper limit of the rate R' without field, the rate R' is found to be 10^{-6} s^{-1} in that case. By comparing both rates, we conclude that the minimum value of the field contribution is $\Delta\epsilon_\mathrm{f} = 0.3$ eV.

For the comparable system of thermal induced hopping of hydrogen on top of one dimer of Si(001), the thermal barrier ϵ was determined experimentally as 1.4 eV [100]. Due to the similarity between the two covalent bonds C-Si and H-Si, a comparable thermal barrier ϵ of 1.4 eV can be assumed for the case of diethyl ether/Si(001). By reconsidering the remaining barrier for the hopping when the electric field is effective, we can estimate the contribution of the field to be $\Delta\epsilon_\mathrm{f}$ =0.5 eV. This indicates that the contribution of the electric field to the hopping events is even stronger than the lower estimated value ($\Delta\epsilon_\mathrm{f}$ >0.3 eV).

The results indicates that the field-induced manipulation on the atomic scale is also possible in the case of covalently bonded entities on semiconductor surfaces. It further demonstrates that the strength of the field has to be in the order of typical values associated with potential energy curve of covalently bonded adsorbates/substrate systems ($\approx$ 1 V/nm) in order to efficiently contribute to the manipulation process.

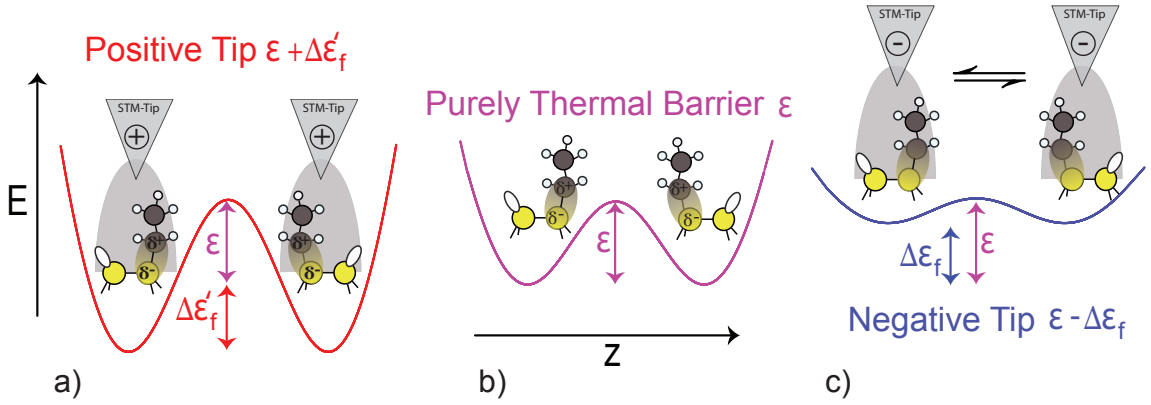

Fig. 3.9: Energetic representation of the two adsorption configurations. The energy barrier ϵ between the two states at room temperature (no bias, b) is either reduced by $\Delta\epsilon_\mathrm{f}$ with positive sample bias (negative tip, c) to become $\epsilon - \Delta\epsilon_\mathrm{f}$, or it is even increased at negative sample bias (positive tip, a) to become $\epsilon + \Delta\epsilon'_\mathrm{f}$.

Bibliography

[1] *Functionalization of Semiconductor Surfaces*, 1 ed., edited by F. Tao and S. Barnasek (John Wiley & Sons, Hoboken, New Jersey, 2012).

[2] I. G. Hill, D. Milliron, J. Schwartz, and A. Kahn, *Organic semiconductor interfaces: electronic structure and transport properties*, Appl. Surf. Sci. **166**, 354 (2000).

[3] J. T. Yates, *A New Opportunity in Silicon-Based Microelectronics*, Science **279**, 335 (1998).

[4] A. H. Flood, J. F. Stoddart, D. W. Steuerman, and J. R. Heath, *Whence Molecular Electronics?*, Science **306**, 2055 (2004).

[5] O. Ostroverkhova, *Organic Optoelectronic Materials: Mechanisms and Applications*, Chem. Rev. **116**, 13279 (2016).

[6] *Organic Optoelectronic Materials*, edited by Y. Li (Springer, Cham, Switzerland, 2015).

[7] M. Lipponer, M. Dürr, and U. Höfer, *Energy dependent sticking coefficients of trimethylamine on Si(001)—Influence of the datively bonded intermediate state on the adsorption dynamics*, Surf. Sci. **651**, 118 (2016).

[8] T. Bohamud, M. Reutzel, M. Dürr, and U. Höfer, *Dynamics of proton transfer reactions on silicon surfaces: OH-dissociation of methanol and water on Si(001)*, J. Chem. Phys. **150**, 224703 (2019).

[9] R. A. Wolkow, *CONTROLLED MOLECULAR ADSORPTION ON SILICON: Laying a Foundation for Molecular Devices*, Annu. Rev. Phys. Chem. **50**, 413 (1999).

[10] R. J. Hamers, S. K. Coulter, M. D. Ellison, J. S. Hovis, D. F. Padowitz, M. P. Schwartz, C. M. Greenlief, and J. N. Russell, *Cycloaddition Chemistry of Organic Molecules with Semiconductor Surfaces*, Acc. Chem. Res. **33**, 617 (2000).

[11] J. Yoshinobu, *Physical properties and chemical reactivity of the buckled dimer on Si(100)*, Prog. Surf. Sci **77**, 37 (2004).

[12] X. Cao, S. K. Coulter, M. D. Ellison, H. Liu, J. Liu, and R. J. Hamers, *Bonding of Nitrogen-Containing Organic Molecules to the Silicon(001) Surface: The Role of Aromaticity*, J. Phys. Chem. B **105**, 3759 (2001).

[13] H. N. Waltenburg and J. T. Yates, *Surface Chemistry of Silicon*, Chem. Rev. **95**, 1589 (1995).

[14] T. Yamaguchi, *Electronic States of Adsorbed Organic Molecule: Pentacene on Si(001)2×1 Surface*, J. Phys. Soc. Jpn. **68**, 1321 (1999).

[15] G. T. Wang, C. Mui, C. B. Musgrave, and S. F. Bent, *Competition and Selectivity of Organic Reactions on Semiconductor Surfaces: Reaction of Unsaturated Ketones on Si(100)-2×1 and Ge(100)-2×1*, J. Am. Chem. Soc **124**, 8990 (2002).

[16] A. J. Carman, L. Zhang, J. L. Liswood, and S. M. Casey, *Methylamine Adsorption on and Desorption from Si(100)*, J. Phys. Chem. B **107**, 5491 (2003).

[17] L. Zhang, A. J. Carman, and S. M. Casey, *Adsorption and Thermal Decomposition Chemistry of 1-Propanol and Other Primary Alcohols on the Si(100) Surface*, J. Phys. Chem. B **107**, 8424 (2003).

[18] T. Kato, S.-Y. Kang, X. Xu, and T. Yamabe, *Possible Dissociative Adsorption of Ch3oh and Ch3nh2 on Si(100)-2 X 1 Surface*, J. Phys. Chem. B **105**, 10340 (2001).

[19] M. Carbone, *α-Amino Thiophene on Si(100)2 X 1: Adsorption and transition states investigated by van der Waals corrected DFT and CI-NEB*, J. Theor. Comput. Chem. **16**, 1740001 (2017).

[20] L. Pecher, S. Schmidt, and R. Tonner, *Modeling the Complex Adsorption Dynamics of Large Organic Molecules: Cyclooctyne on Si(001)*, J. Phys. Chem. C **121**, 26840 (2017).

[21] M. Gallo, E. Martínez-Guerra, and J. A. Rodríguez, *Growth of Acetone Molecular Lines on the Si(001)(2×1)–H Surface: First-Principle Calculations*, J. Phys. Chem. C **116**, 20292 (2012).

[22] M. A. Filler and S. F. Bent, *The surface as molecular reagent: organic chemistry at the semiconductor interface*, Prog. Surf. Sci. **73**, 1 (2003).

[23] T. R. Leftwich and A. V. Teplyakov, *Chemical manipulation of multifunctional hydrocarbons on silicon surfaces*, Surf. Sci. Rep. **63**, 1 (2008).

[24] A. Racis, L. Jurczyszyn, M. Bazarnik, W. Koczorowski, A. Wykrota, R. Czajka, and M. W. Radny, *Self-organisation of inorganic elements on Si(001) mediated by pre-adsorbed organic molecules*, Phys. Chem. Chem. Phys. **17**, 23783 (2015).

[25] O. Warschkow, I. Gao, S. R. Schofield, D. R. Belcher, M. W. Radny, S. A. Sarairehc, and P. V. Smithc, *Acetone on silicon (001): ambiphilic molecule meets ambiphilic surface*, Phys. Chem. Chem. Phys. **11**, 2747 (2009).

[26] J. Owen, *Competing interactions in molecular adsorption: NH3on Si(001)*, J. Phys.-Condens. Mat. **21**, 443001 (2009).

[27] J.-H. Cho and L. Kleinman, *Adsorption of cyclopentene on the Si(001) surface: A first-principles study*, Phys. Rev. B **64**, 235420 (2001).

[28] X. Peng, P. Krüger, and J. Pollmann, *Adsorption processes of hydrogen molecules on SiC(001), Si(001) and C(001) surfaces*, New J. Phys. **10**, 125028 (2008).

[29] G. Mette, M. Reutzel, R. B. S. Laref, R. Tonner, M. Dürr, U. Koert, and U. Höfer, *Complex surface chemistry of an otherwise inert solvent molecule: tetrahydrofuran on Si(001)*, ChemPhysChem **15**, 3725 (2014).

[30] G. Mette, M. Dürr, R. Bartholomäus, U. Koert, and U. Höfer, *Real-space adsorption studies of cyclooctyne on Si(001)*, Chem. Phys. Lett. **556**, 70 (2013).

[31] G. Mette, C. H. Schwalb, M. Dürr, and U. Höfer, *Site-selective reactivity of ethylene on clean and hydrogen precovered Si(001)*, Chem. Phys. Lett. **483**, 209 (2009).

[32] M. Reutzel, G. Mette, P. Stromberger, U. Koert, M. Dürr, and U. Höfer, *Dissociative adsorption of diethyl ether on Si(001) studied by means of scanning tunneling microscopy and photoelectron spectroscopy*, J. Phys. Chem. C **119**, 6018 (2015).

[33] M. Dürr and U. Höfer, *Dissociative adsorption of molecular hydrogen on silicon surfaces*, Surf. Sci. Rep. **61**, 465 (2006).

[34] N. Takeuchi, Y. Kanai, and A. Selloni, *Surface Reaction of Alkynes and Alkenes with H-Si(111): A Density Functional Theory Study*, J. Am. Chem. Soc **126**, 15890 (2004).

[35] C.-Y. Niu and J.-T. Wang, *Adsorption and dissociation of oxygen molecules on Si(111)-(7×7) surface*, J. Chem. Phys. **139**, 194709 (2013).

[36] M. T. Yin and M. L. Cohen, *Theoretical determination of surface atomic geometry: Si(001)-(2×1)*, Phys. Rev. B **24**, 2303 (1981).

[37] H. Nakayama, T. Nishino, K. Ueda, S. Takeno, and H. Fujita, *Surface wave excitation Auger electron spectroscopy of Si(001) reconstructed surfaces*, Ultramicroscopy **39**, 329 (1991).

[38] D. J. Chadi, *Atomic and Electronic Structures of Reconstructed Si(100) Surfaces*, Phys. Rev. Lett. **43**, 43 (1979).

[39] P. Krüger and J. Pollmann, *Dimer Reconstruction of Diamond, Si, and Ge (001) Surfaces*, Phys. Rev. Lett. **74**, 1155 (1995).

[40] A. Groß, *Reactions at surfaces studied by ab initio dynamics calculations*, Surf. Sci. Rep. **32**, 291 (1998).

[41] G. R. Darling and S. Holloway, *The dissociation of diatomic molecules at surfaces*, Rep. Prog. Phys. **58**, 1595 (1995).

[42] M. Lipponer, M. Dürr, and U. Höfer, *Adsorption dynamics of tetrahydrofuran on Si(001) studied by means of molecular beam techniques*, Chem. Phys. Lett. **624**, 69 (2015).

[43] M. Reutzel, M. Lipponer, M. Dürr, and U. Höfer, *Binding energy and dissociation barrier - experimental determination of the key parameters of the potential energy curve of diethyl ether on Si(001)*, J. Phys. Chem. Lett. **6**, 3971 (2015).

[44] M. Dürr, M. B. Raschke, and U. Höfer, *Effect of beam energy and surface temperature on the dissociative adsorption of H_2 on Si(001)*, J. Chem. Phys. **111**, 10411 (1999).

[45] M. Dürr and U. Höfer, *Molecular beam investigation of hydrogen dissociation on Si(001) and Si(111) surfaces*, J. Chem. Phys. **121**, 8058 (2004).

[46] *Atomic and Molecular Beam Methods*, edited by G. Scoles (Oxford University Press, Oxford, 1988).

[47] S. DePaul, D. Pullman, and B. Friedrich, *A pocket model of seeded supersonic beams*, J. Phys. Chem. **97**, 2167 (1993).

[48] M. A. Lipponer, *Untersuchungen zur Adsorptionsdynamik von Tetrahydrofuran, Trimethylamin und Cyclooctin auf Silizium-(001)*, Dissertation, Philipps-Universität Marburg, 2014.

[49] D. A. King and M. G. Wells, *Molecular beam investigation of adsorption kinetics on bulk metal targets: Nitrogen on tungsten*, Surf. Sci. **29**, 454 (1972).

[50] T. Takaoka and I. Kusunoki, *Sticking probability and adsorption process of NH3 on Si(100) surface*, Surf. Sci. **412-413**, 30 (1998).

[51] G. Binnig, H. Rohrer, Ch. Gerber, and E. Weibel, *Surface Studies by Scanning Tunneling Microscopy*, Phys. Rev. Lett. **49**, 57 (1982).

[52] O. M. Magnussen, J. Hotlos, R. J. Nichols, D. M. Kolb, and R. J. Behm, *Atomic structure of Cu adlayers on Au(100) and Au(111) electrodes observed by in situ scanning tunneling microscopy*, Phys. Rev. Lett. **64**, 2929 (1990).

[53] *Introduction to Scanning Tunneling Microscopy: Second Edition*, edited by J. Chen (Oxford University Press, Oxford, 2012).

[54] J. Bardeen, *Tunnelling from a Many-Particle Point of View*, Phys. Rev. Lett. **6**, 57 (1961).

[55] G. Mette, *Untersuchungen zur selektiven Reaktivität von Ethen, Cyclooctin und Tetrahydrofuran mit Si(001)-Oberflächen*, Dissertation, Philipps-Universität Marburg, 2012.

[56] R. J. Hamers, *Atomic-Resolution Surface Spectroscopy with the Scanning Tunneling Microscope*, Annu. Rev. Phys. Chem. **40**, 531 (1989).

[57] W. Ho, *Single-molecule chemistry*, J. Chem. Phys. **117**, 11033 (2002).

[58] R. Otero, F. Rosei, and F. Besenbacher, *Scanning tunneling microscopy manipulation of complex organic molecules on solid surfaces*, Annu. Rev. Phys. Chem. **57**, 497 (2006).

[59] Y. Kim, K. Motobayashi, T. Frederiksen, H. Ueba, and M. Kawai, *Action spectroscopy for single-molecule reactions - Experiments and theory*, Prog. Surf. Sci. **90**, 85 (2015).

[60] J. Oh, H. Lim, R. Arafune, J. Jung, M. Kawai, and Y. Kim, *Lateral Hopping of CO on Ag(110) by Multiple Overtone Excitation*, Phys. Rev. Lett. **116**, 056101 (2016).

[61] G. Dujardin, E. B. Duchemin, E. Le. Moal, A. J. Mayne, and D. Riedel, *DIET at the nanoscale*, Surf. Sci. **643**, 13 (2016).

[62] O. MacLean, K. Huang, L. Leung, and J. C. Polanyi, *Direct and Delayed Dynamics in Electron-Induced Surface Reaction*, J. Am. Chem. Soc. **139**, 17368 (2017).

[63] N. Okabayashi, A. Peronioa, M. Paulssonc, T. Arai, and F. J. Giessibl, *Vibrations of a molecule in an external force field*, Proc. Natl. Acad. Sci. U.S.A **115**, 4571 (2018).

[64] E. Kazuma, J. Jung, H. Ueba, M. Trenary, and Y. Kim, *Real-space and real-time observation of a plasmon-induced chemical reaction of a single molecule*, Science **360**, 521 (2018).

[65] K. R. Rusimova, R. M. Purkiss, R. Howes, F. Lee, S. Crampin, and P. A. Sloan, *Regulating the femtosecond excited-state lifetime of a single molecule*, Science **361**, 1012 (2018).

[66] L. Bartels, G. Meyer, and K.-H. Rieder, *Basic Steps of Lateral Manipulation of Single Atoms and Diatomic Clusters with a Scanning Tunneling Microscope Tip*, Phys. Rev. Lett. **79**, 697 (1997).

[67] G. Mette, A. Adamkiewicz, M. Reutzel, M. Dürr, and U. Höfer, *Controlling an SN2 Reaction by Electronic and Vibrational Excitation: Tip-Induced Ether Cleavage on Si(001)*, Angew. Chem. Int. Ed. **58**, 3417 (2019).

[68] T.-C. Shen and P. Avouris, *Electron stimulated desorption induced by the scanning tunneling microscope*, Surf. Sci **390**, 35 (1997).

[69] T.-C. Shen, C. Wang, G. C. Abein, J. R. Tucker, J. W. Lyding, P. Avouris, and R. E. Walkup, *Atomic-Scale Desorption Through Electronic and Vibrational Excitation Mechanisms*, Science **268**, 1590 (1995).

[70] B. C. Stipe, M. A. Rezaei, and W. Ho, *Inducing and Viewing the Rotational Motion Of a Single Molecule*, Science **279**, 1907 (1998).

[71] J. A. Stroscio and D. M. Eigler, *Atomic and Molecular Manipulation with the Scanning Tunneling Microscope*, Science **254**, 1319 (1991).

[72] I.-W. Lyo and P. Avouris, *Field-Induced Nanometer- to Atomic-Scale Manipulation of Silicon Surfaces with the STM*, Science **253**, 173 (1991).

[73] M. Alemani, M. V. Peters, S. Hecht, K.-H. Rieder, F. Moresco, and L. Grill, *Electric Field-Induced Isomerization of Azobenzene by STM*, J. Am. Chem. Soc **128**, 14446 (2006).

[74] J. Calupitan, O. Galangau, O. Guillerme, R. Coratger, T. Nakashima, O. Rapenne, and O. Kawai, *Scanning Tunneling Microscope Tip-Induced Formation of a Supramolecular Network of Terarylene Molecules on Cu(111)*, J. Phys. Chem. C **121**, 25384 (2017).

[75] S. Rogge, R. H. Timmerman, P. M. L. O. Scholte, L. J. Geerligs, and H. W. M. Salemink, *Field-based scanning tunneling microscope manipulation of antimony dimers on Si(001)*, J. Vac. Sci. Technol. **19**, 659 (2001).

[76] M. A. Rezaei, B. C. Stipe, and W. Ho, *Atomically resolved adsorption and scanning tunneling microscope induced desorption on a semiconductor: NO on Si(111)-(7×7)*, J. Chem. Phys **110**, 4891 (1999).

[77] M. Bowker, *The Role of Precursor States in Adsorption, Surface Reactions and Catalysis*, TOP. CATAL. **59**, 663 (2016).

[78] M. A. Lipponer, N. Armbrust, M. Dürr, and U. Höfer, *Adsorption dynamics of ethylene on Si(001)*, J. Phys. Chem. **136**, 144703 (2012).

[79] P. Kisliuk, *The sticking probabilities of gases chemisorbed on the surfaces of solids*, J. Phys. Chem. Solids **3**, 95 (1957).

[80] C. Länger, T. Bohamud, J. Heep, T. Glaser, M. Reutzel, U. Höfer, and M. Dürr, *Adsorption of Methanol on Si(001): Reaction Channels and Energetics*, J. Phys. Chem. C **122**, 14756 (2018).

[81] X. Lu, Q. Zhang, and M. C. Lin, *Adsorption of methanol, formaldehyde and formic acid on the Si(100)-2 × 1 surface: A computational study*, Phys. Chem. Chem. Phys. **3**, 2156 (2001).

[82] P. L. Silvestrelli, *Adsorption of ethanol on Si(100) from first principles calculations*, Surf. Sci. **552**, 17 (2004).

[83] C. Mui, J. H. Han, G. T. Wang, C. B. Musgrave, and S. F. Bent, *Proton Transfer Reactions on Semiconductor Surfaces*, J. Am. Chem. Soc **124**, 4027 (2002).

[84] C.-H. Chung, W.-J. Jung, and I.-W. Lyo, *Trapping-Mediated Chemisorption of Ethylene on* Si(001)$-c(4 \times 2)$, Phys. Rev. Lett. **97**, 116102 (2006).

[85] C. Länger, J. Heep, P. Nikodemiak, T. Bohamud, P. Kirsten, U. Höfer, U. Koert, and M. Dürr, *Formation of Si/organic interfaces using alkyne-functionalized cyclooctynes—precursor-mediated adsorption of linear alkynes versus direct adsorption of cyclooctyne on Si(0 0 1)*, J. Phys.-Condens. Mat. **31**, 034001 (2019).

[86] J.-H. Cho and L. Kleinman, *Adsorption kinetics of acetylene and ethylene on Si(001)*, Phys. Rev. B **69**, 075303 (2004).

[87] J. Pecher, G. Mette, M. Dürr, and R. Tonner, *Site-Specific Reactivity of Ethylene at Distorted Dangling-Bond Configurations on Si(001)*, ChemPhysChem **18**, 357 (2016).

[88] M. Reutzel, N. Münster, M. Lipponer, C. Länger, U. Höfer, U. Koert, and M. Dürr, *Chemoselective Reactivity of Bifunctional Cyclooctynes on Si(001)*, J. Phys. Chem. C **120**, 26284 (2016).

[89] O. Warschkow, S. R. Schofield, N. A. Marks, M. W. Radny, P. V. Smith, and D. R. McKenzie, *Water on silicon (001): C defects and initial steps of surface oxidation*, Phys. Rev. B **77**, 201305 (2008).

[90] J.-H. Cho, K. S. Kim, S.-H. Lee, and M.-H. Kang, *Dissociative adsorption of water on the Si(001) surface: A first-principles study*, Phys. Rev. B **61**, 4503 (2000).

[91] L. J. Lauhon and W. Ho, *Single-Molecule Chemistry and Vibrational Spectroscopy: Pyridine and Benzene on Cu(001)*, J. Phys. Chem. A **104**, 2463 (2000).

[92] R. M. Purkiss, H. G. Etheridge, P. A. Sloan, and K. R. Rusimova, *Common source of light emission and nonlocal molecular manipulation on the Si(111)-*(7×7), J. Phys. Commun. **3**, 095010 (2019).

[93] P. A. Sloan, S. Sakulsermsuk, and R. E. Palmer, *Nonlocal Desorption of Chlorobenzene Molecules from the Si(111)-*(7×7) *Surface by Charge Injection from the Tip of a Scanning Tunneling Microscope: Remote Control of Atomic Manipulation*, Phys. Rev. Lett. **105**, 048301 (2010).

[94] C. Girard, C. Joachim, C. Chavy, and P. Sautet, *The electric field under a STM tip apex: implications for adsorbate manipulation*, Surf. Sci. **282**, 400 (1993).

[95] T. M. Mayer, D. P. Adams, and B. M. Marder, *Field emission characteristics of the scanning tunneling microscope for nanolithography*, J. Vac. Sci. Technol. **14**, 2438 (1996).

[96] S. V. Snegir, P. Yu, F. Maurel, O. L. Kapitanchuk, A. A. Marchenko, and E. Lacaze, *Switching at the Nanoscale: Light- and STM-Tip-Induced Switch of a Thiolated Diarylethene Self-Assembly on Au(111)*, Langmuir **30**, 13556 (2014).

[97] D. V. Potapenko, Z. Li, and R. M. Osgood, *Dissociation of Single 2-Chloroanthracene Molecules by STM-Tip Electron Injection*, J. Phys. Chem. C **116**, 4679 (2012).

[98] S. Katano, Y. Kim, Y. Kagata, and M. Kawai, *Single-Molecule Vibrational Spectroscopy and Inelastic-Tunneling-Electron-Induced Diffusion of Formate Adsorbed on Ni(110)*, J. Phys. Chem. C **114**, 3003 (2010).

[99] O. Bikondoa, C. L. Pang, R. Ithnin, C. A. Muryn, H. Onishi, and G. Thornton, *Direct visualization of defect-mediated dissociation of water on TiO2(110)*, Nat. Mater. **5**, 189 (2006).

[100] M. Dürr and U. Höfer, *Hydrogen diffusion on silicon surfaces*, Prog. Surf. Sci. **88**, 61 (2013).

List of Figures

List of Publications

I Adsorption of Methanol on Si(001): Reaction Channels and Energetics
C. Länger, *T. Bohamud*, J. Heep, T. Glaser, M. Reutzel, U. Höfer, and M. Dürr;
J. Phys. Chem. C **122**, 14756-14760 (2018).

II Formation of Si/organic interfaces using alkyne-functionalized cyclooctynes -precursor-mediated adsorption of linear alkynes versus direct adsorption of cyclooctyne on Si(001)
C. Länger, J. Heep, P. Nikodemiak, *T. Bohamud*, P. Kirsten, U. Höfer, U. Koert and M. Dürr;
J. Phys.-Condens. Mat. **31**, 034001 (2019).

III Dynamics of proton transfer reactions on silicon surfaces: OH- dissociation of methanol and water on Si(001)
T. Bohamud, M. Reutzel, M. Dürr, and U. Höfer;
J. Chem. Phys. **150**, 3224703 (2019).

IV Electric Field Induced Depolarization of Si-C Bond Leads to Strongly Reduced Barrier for Alkyl-Hopping on Si(001)
T. Bohamud, M. Reutzel, A. Adamkiewicz, U. Höfer, and M. Dürr;
J. Phys. Chem. C **124**, 5270–5274 (2020).

Wissenschaftlicher Werdegang

10/2002 –10/2005	Studium der Drahtlose Kommunikationstechnologie
10/2005–10/2010	Studium der Physik an der Universität Damaskus
10/2010	Bachelor of Science, Physics
10/2012–05/2015	Studium der Physik an der Universität Rostock
06/2015	Master-Thesis in der Arbeitsgruppe Oberflächendynamik bei Prof. Dr. Frau S. Speller: *Plasmonic Nanoparticles Prepared by Nanosphere Lithography for Local Excitation of Molecular Aggregates*
06/2012	Master of Science, Physics
11/2015–10/2018	Stipendiat des Graduiertenkolleges *Funktionalisierung von Halbleitern*, (GRK 1782)
11/2018–heute	Wissenschafltlicher Mitarbeiter an der Arbeitsgruppe Oberflächenphysik Doktorvater: Prof. Dr. U. Höfer *Non-Thermal Activation of Reactions of Organic Molecules on Si(001)-Molecular Beam and Scanning Tunneling Microscopy Experiments*

Acknowledgment

I would like to give my deep gratitude to the people who have helped to accomplish this work.
First of all, I would like to thank Prof. Dr. Ulrich Höfer for accepting me in his work group, and for the continuous guidance and advising.
Many special thanks are given to Prof. Dr. Michael Dürr for the great help in accomplishing this work and for being always available for my questions, and for the weekly profound discussions about the results and for the assistance in the labs.
I thank Dr. Marcel Reutzel for his considerable contribution to this work and for the guidance during the first stages of the research.
I thank the DFG (*Deutsche Forschungsgemeinschaft*) for the financial support within the framework of GRK 1782 and SFB 1083, and I thank the University of Giessen for the finance during the very last stage of the work.
I thank Dr. Gerson Mette and Prof. Dr. Jens Güdde for providing me with their important ideas about solving many difficult problems.
Last but not the least, I would like to extend my special words of appreciation to the members of the work group of surface science at the university of Marburg: Alexa Adamkiewicz, Sarah Zajusch, Marleen Axt, Steven Youngkin, Jonas Zimmermann, Dr. Johannes Reimann, Dr. Suguru Ito, Lasse Münster, Dr. Nico Armbrust, Dr. Alexander Lerch, Dr. Andreas Namgalies, Dr. Klaus Stallberg, Dr. Reza Kakavandi, our secretariat represented by Irene Dippel-Hauser and Dr. Helen A. Pfuhl, the mechanical and electronic workshop of department of physics in Marburg represented by Mr. Manfred Preis, Mr. Hermann Günther, Mr. Rainer Täubner, Dipl.-Ing. Carsten Schindler. I was lucky to be in your environment for 4 years and to had the chance to learn from you.